Chaos, Solitons & Fractals 55 (2013) 102–108

Contents lists available at SciVerse ScienceDirect

Chaos, Solitons & Fractals

Nonlinear Science, and Nonequilibrium and Complex Phenomena

journal homepage: www.elsevier.com/locate/chaos

Strobing brain thunders: Functional correlation of extreme activity events

F. Lombardi [a], D.R. Chialvo [b], H.J. Herrmann [a,d], L. de Arcangelis [c,*]

[a] Institute Computational Physics for Engineering Materials, ETH, Zürich, CH, Switzerland
[b] Consejo Nacional de Investigaciones Científicas y Tecnológicas, CONICET, Buenos Aires, Argentina
[c] Dept. of Industrial and Information Engineering, Second University of Naples and INFN Gr. Coll. Salerno, Aversa (CE), Italy
[d] Departamento de Física, Universidade Federal do Ceará, Fortaleza 60451-970, Ceará, Brazil

ARTICLE INFO

Article history:
Available online 10 July 2013

ABSTRACT

The recent upraise of interest in the dynamics of the brain resting activity opens a number of new and different questions. A fundamental one is related to the character of correlations of healthy large scale brain activity. These studies focus on the linear correlation of the spontaneous activity between brain sites. Here we present a different approach, instead to estimate the average linear correlation of activity between pairs of brain sites, we ask: what are average sequels in space and time of a big event (i.e., a thunder). By strobing these events we find that on average the activity variations with opposite sign are correlated in time, over a temporal scale of few seconds, exposing a critical balance between excitation and depression opposing forces.

1. Introduction

An increasing number of reports deals with spontaneous brain dynamics at large scale. It is known that the brain activity at this coarse scale organizes into relatively few spatio-temporal patterns, as revealed experimentally in recent years [1]. A wide range of experiments using functional Magnetic Resonance Imaging (fMRI) have emphasized that these spatial clusters of coherent activity, termed Resting State Networks (RSN) [2], are specifically associated with neuronal systems responsible for sensory, cognitive and behavioral functions [3]. Furthermore, the pattern of correlations in these networks has been shown to change with various cognitive and pathophysiological conditions [1]. At the same time studies have shown that the RSN activity exhibits peculiar scaling properties, resembling dynamics near the critical point of a second order phase transition [4–6], consistent with evidence showing that the brain at rest is near a critical point [7]. More precisely, these empirical findings are in line with experimental results on spontaneous activity in cortical systems in vitro and in vivo [8–10] and with computational modeling results [11–18]. Indeed, spontaneous neuronal activity generally exhibits slow oscillations between bursty periods, followed by substantially quiet periods. Bursts can last from a few to several hundreds of milliseconds and, if analyzed at a finer temporal scale, show a complex structure in terms of neuronal avalanches. In vitro experiments allow to record avalanche activity [8,19] from mature organotypic cultures of rat somatosensory cortex where they spontaneously emerge in superficial layers. The size and duration of neuronal avalanches follow power law distributions with very stable exponents, which is a typical feature of a system acting in a critical state, where large fluctuations are present and the response does not have a characteristic size. The same critical behavior has been measured also in vivo from rat cortical layers during early post-natal development [20], from the cortex of awake adult rhesus monkeys [10], using microelectrode array recordings, as well as for dissociated neurons from rat hippocampus [21,22] or leech ganglia [21]. Operating at a critical level, far from an uncorrelated subcritical or a too correlated supercritical regime, may optimize information

* Corresponding author. Tel.: +39 0815010249.
E-mail address: lucilla.dearcangelis@unina2.it (L. de Arcangelis).

0960-0779/$ - see front matter © 2013 Elsevier Ltd. All rights reserved.
http://dx.doi.org/10.1016/j.chaos.2013.06.003

management and transmission in real brains, as recently confirmed by experiments [23].

The emergence of power law distributions has been interpreted in terms of self-organized criticality (SOC) [4]. The term SOC usually refers to a mechanism of slow energy accumulation and fast energy redistribution driving the system toward a critical state, where the avalanche extensions and durations follow power law distributions. The simplicity of the mechanism at the basis of SOC has suggested that many physical and biological phenomena characterized by power laws in the size distribution represent natural realizations of the SOC idea. For instance, SOC has been proposed to model earthquakes [24,25], the evolution of biological systems [26], solar flare occurrence [27], fluctuations in confined plasma [28], snow avalanches [29], and rainfall [30]. Understanding the brain electrical activity at large scale is a fundamental issue, which cannot be derived from the abundance of information at the microscopic level. As an analogy, weather forecasting hardly could be inferred from local data in the absence of a good model of large scale atmosphere dynamics.

This special issue is dedicated to our colleague and friend Werner who knew first-hand how important the global picture can be to understand the brain. In multiple occasions in the last years of his long tenure as a brilliant physiologist he insisted on the importance of applying concepts coming from different fields to the understanding of brain dynamics. In particular, Werner adopted in his studies methods coming from critical phenomena and complex systems [31] noticing that "the molecular rearrangement becomes at the macroscopic level manifest as a set of qualitatively new properties that could not be deduced from the microscopic state change, nor could it be anticipated from the prior macroscopic state" [32]. This interdisciplinary approach indeed represents a conceptual framework able to provide new insights into brain dynamics.

The interest for mesoscopic brain dynamics is not new, of course. It is inspiring to read that the father of brain modeling Warren McCulloch, more than 60 years ago, was concerned with the same issues than Werner and us today. Together with Dusser de Barenne, Warren McCulloch and colleagues [36,37] experimented inducing local seizures by applying small drops of strychnine in several regions of the monkey cortex while recording cortical electrical activity simultaneously in twenty sites across the entire cortex. This clever technique, mastered by Dusser de Barenne, received the name of strychnine neuronography, which can be considered the earliest attempt to study brain functional connectivity, by inducing some liminal activity in a given area and recording the co-active cortical sites. Typically, they noticed that the initial activity induced by the strychnine remained local, and did not spread to the entire cortex. However, not without surprise, they noted that, less often, the activity was recorded in very far away locations.

Fig. 1 (redrawn from the original sketches in [35]) summarizes these early observations together with our own rough estimations in Panel D. Filled circles in Panel D represent the distribution of edge lengths, computed from the drawing in Panel A as the Euclidean distance (using arbitrary units) between the location of each strychnine instillation and the resulting activation site/s. Note that, despite the scarcity of the data, the results demonstrate long range correlations, the exponent being similar to the estimations using fMRI [34]. For example an application in the frontal cortex induced sometimes activity as far as to the occipital cortex. Nowadays, is not difficult to admit that frontal activation will evoke visual images and vice versa, however McCulloch knew that much before us.

2. Conditional probability approach

Here we present a statistical analysis of experimental data of functional magnetic resonance inspired by a novel interdisciplinary approach: we apply a method developed to detect correlations in magnitude, time and spatial location between successive earthquakes [38] in seismic catalogs. This analysis is very difficult to perform since statistical noise hides the presence of correlations. The method, comparing probabilities evaluated in the real catalog with a catalog made uncorrelated by reshuffling, is able to subtract the effect of noise. Our aim is to investigate the existence and features of spatio-temporal correlations in activity variations. More precisely, the analysis aims at enlightening the structure of these correlations and their relationship with the spatial and temporal distance between successive variations. The study focuses on correlations between large events, analogously to a recent work [39] that analyzed the gradual and continuous changes in the brain blood oxygenated level dependent (BOLD) signal to estimate functional connectivity from resting BOLD events triggered average. The activity $B(\vec{r}_i, t)$ is monitored at each voxel i as function of time. Data are recorded in time every $\delta t = 2.5$ s, therefore time is measured in unit of δt. We focus our study only on extreme activity events (thunders) and therefore analyze voxels for which $B(\vec{r}_i, t)$ is larger than a given threshold B_c = 18,000, value that selects the largest 10% of the entire activity range. Namely, we substitute the below-threshold values with zero and leave the above-threshold values of $B(\vec{r}_i, t)$ unchanged. The local activity variations at each voxel are evaluated as $s_i(t) = B(\vec{r}_i, t + \delta t) - B(\vec{r}_i, t)$, which can have positive and negative values. As a first attempt, we simply calculate the average cross-correlation function on the entire set of data as

$$G(\tau) = \overline{\langle (s_i(t+\tau) - \overline{s_i(t)})(s_j(t+\tau) - \overline{s_j(t)}) \rangle} \qquad (1)$$

where the bar indicates the temporal average, whereas brackets stand for the average over all possible voxel couples. In order to evaluate the role of statistical noise on this quantity, we calculate $G(\tau)$ also in a catalog where $s_i(t)$ values are reshuffled in time and space. In this way, the data set we generate is uncorrelated by construction and therefore should show a cross-correlation function fluctuating around zero. The amplitude of fluctuations is a measure of the statistical noise present in the catalog. In Fig. 2 we plot $G(\tau)$ for both data sets. In the original catalog the cross-correlation exhibits strong fluctuations over a range comparable to the one measured in the uncorrelated data set. It is therefore quite difficult to extract information on

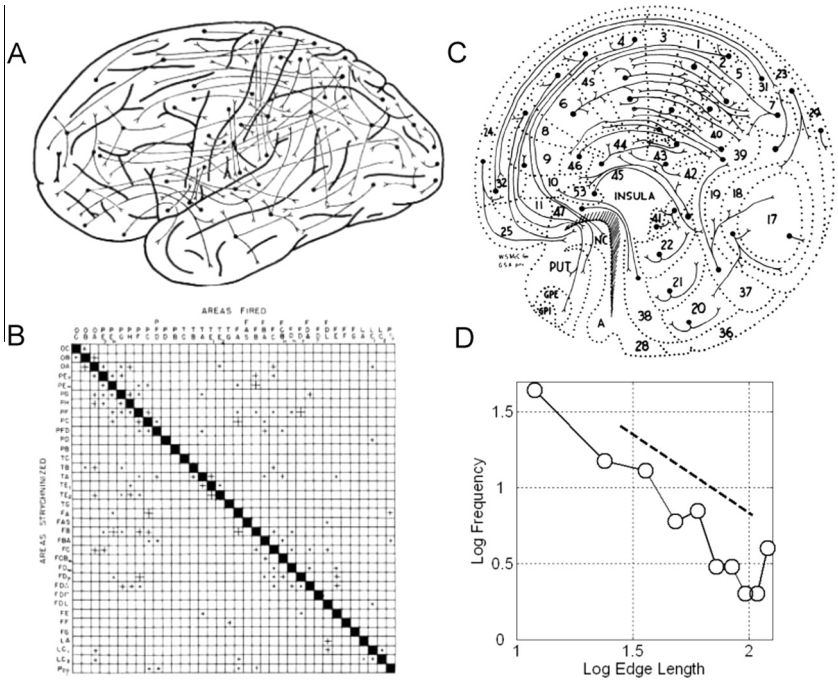

Fig. 1. McCulloch experiments inducing local seizures by instillation of strychnine. Panel A and B are from chimpanzee experiments [35]. Panel A shows a summary of the sites where the strychnine was applied (filled circled) and the sites of the cortex which fired by the topical application. Besides the local ones, long range activations crossing the entire cortex were often observed. Panel B illustrates the adjacency matrix summarizing which areas – on average – were activated by the strychnine application. Panel C shows similar results obtained by McCulloch and colleagues in Macaca Mulata [37] mapping the entire cortex and basal ganglia. Panel D depicts (note the double logarithmic axis) the edge length density distribution computed from McCulloch's drawing in Panel A. The dashed line with slope 2 illustrates, for comparison, the average edge-length density found in recent fMRI experiments [34]. Reproduced from [33].

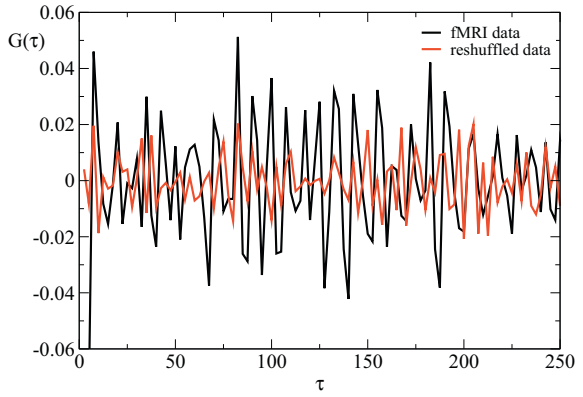

Fig. 2. Cross-correlation function for the variations in the experimental data set (black line) and in the data set generated by reshuffling the original data over time and voxels (red line). (For interpretation of the references to color in this figure legend, the reader is referred to the web version of this article.)

correlations by a direct measurement from the original experimental catalog.

We describe here the recent statistical method developed to analyze correlations in seismic catalogs [38]. The basic idea of the method is to compare the behavior of conditional probabilities evaluated in an experimental catalog and in a synthetic catalog containing the same data but reshuffled in time and space. In such catalog, by definition, eventual spatio-temporal correlations are destroyed. We analyze the temporal series of $s_i(t)$. We define the quantity $\Delta t = t' - t > 0$ as the temporal distance between two variations occurring at times t and t', which can assume values from 1 to 400 in units of $\delta t = 2.5$ s. Analogously, we define the Euclidean distance between two voxels l and m as $\Delta r = \mid \vec{r}_l - \vec{r}_m \mid$, where $\vec{r}$ is the three dimensional position of the center of a voxel. Furthermore, we define $\Delta s = s_l(t') - s_m(t)$ as the difference between variations occurring at a temporal distance Δt at any couple of voxels l, m whose spatial distance is Δr. We also evaluate $\Delta s^* = s_l(t') - s^*_m(t^*)$ where s^* is value of s taken at random in the entire series. This quantity corresponds to the difference in deviations between any couple of voxels in a catalog where the entire series $s_i(t)$ is reshuffled in time and voxels. Hence, Δs^* is the difference of variations within a catalog where a variation is uncorrelated to previous ones by construction.

We then define the conditional probability

$$P(\Delta x < x_0 \mid \Delta y < y_0) \equiv \frac{N(x_0, y_0)}{N(y_0)} \tag{2}$$

where $N(x_0, y_0)$ is the number of couples of subsequent events with both $\Delta x < x_0$ and $\Delta y < y_0$ and $N(y_0)$ is the number of couples with $\Delta y < y_0$. In the following Δx or Δy will be used to indicate, depending on cases, $\Delta r, \Delta t, \Delta s$ or Δs^*. Our method is schematically presented in Fig. 3.

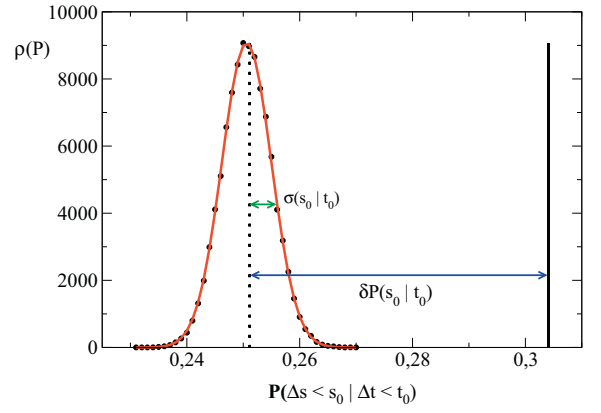

Fig. 3. The distribution $\rho(P)$ of $P(\Delta s^* < s_0 \mid \Delta t < t_0)$ for $t_0 = 5$ s and $s_0 = 0$ (black circles) evaluated for 10^5 configurations of the reshuffled catalog. $\rho(P)$ is well fitted by a Gaussian (red line) with mean value $Q(s_0, t_0) = 0.2511$ and standard deviation $\sigma(s_0, t_0) = 0.0044$. The evaluation of $P(\Delta s < s_0 \mid \Delta t < t_0)$ for the same s_0 and t_0 in the real catalog (black line) provides the value 0.3041. As a consequence $\delta P(s_0, t_0) = 0.0530 \simeq 12.0\sigma(s_0, t_0)$. (For interpretation of the references to color in this figure legend, the reader is referred to the web version of this article.)

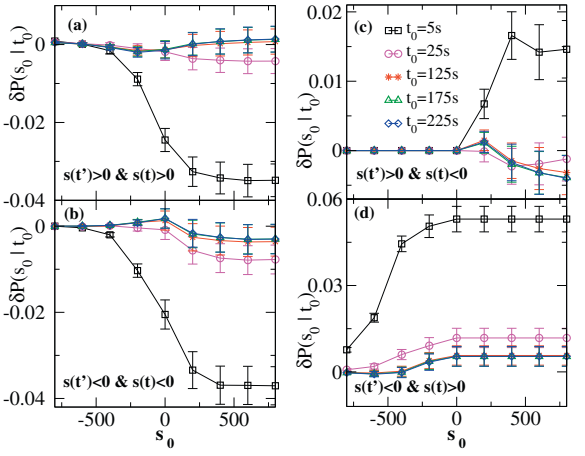

Fig. 4. The quantity $\delta P(s_0, t_0)$ as a function of s_0 for $t_0 = 5$, 25, 125, 175, 225 s. For each t_0 and s_0 the error bar is the standard deviation $\sigma(s_0, t_0)$. Different panels consider all possible combinations of sign of successive variations.

Keeping s_0 and t_0 fixed, we compute the quantity $P(\Delta s^* < s_0 \mid \Delta t < t_0)$ for several independent random realizations of the reshuffled catalog, obtaining the distribution $\rho[P(\Delta s^* < s_0 \mid \Delta t < t_0)]$. Taking 10^5 independent realizations of the variation reshuffling, for each s_0 and t_0, we find that $\rho[P(\Delta s^* < s_0 \mid \Delta t < t_0)]$ is Gaussian distributed with mean value $Q(s_0, t_0)$ and standard deviation $\sigma(s_0, t_0)$. Analogous behavior is obtained for $P(\Delta s^* < s_0 \mid \Delta r < r_0)$ and we similarly define $Q(s_0, r_0)$ and $\sigma(s_0, r_0)$. The relevant quantity is $\delta P(s_0, y_0) = P(\Delta s < s_0 \mid \Delta y < y_0) - Q(s_0, y_0)$, i.e., the difference between the value of $P(\Delta s < s_0 \mid \Delta y < y_0)$ in the real catalog and its mean value in reshuffled catalogs. If the absolute value $\mid \delta P(s_0, y_0) \mid$ is different than zero, a significant difference in the number of couples satisfying both conditions exists between the real and the random series. In particular, if $\mid \delta P(s_0, y_0) \mid$ is larger than zero it is more likely to find couples of data satisfying both conditions in the real rather than in the random catalog. Since in the random catalog correlations are destroyed by construction and only statistical noise affects the data, the difference in conditional probabilities is due to physical correlations in voxel activity. In our analysis, we conclude that significant non-zero correlations between magnitudes of successive variations exist if $\mid \delta P(s_0, y_0) \mid > \sigma(s_0, y_0)$.

In Fig. 3 we explicitly compare $\rho[P(\Delta s^* < s_0 \mid \Delta t < t_0)]$ with $P(\Delta s < s_0 \mid \Delta t < t_0)$ for $s_0 = 0$ and $t_0 = 5$ s. We clearly observe the existence of non-zero correlations, since $\delta P(s_0, t_0) \simeq 12.0\sigma(s_0, t_0)$. For a deeper understanding of the nature of the observed correlations, the above analysis has been extended to different values of s_0, r_0 and t_0.

In Fig. 4 we plot the $\delta P(s_0, t_0)$ as a function of s_0 for different values of t_0. The error bar of each point is the standard deviation $\sigma(s_0, t_0)$ defined above. To have a finer understanding of the features of temporal correlations we analyze separately the four different cases: (a) the successive local variations are both positive, (b) both negative and (c,d) have different signs. These are independent of each other and the total probability is the superposition of the different cases. We notice that the number of couples in the denominator of Eq. (2) is the same for each case. We first discuss the case of successive variations with the same sign ((a) and (b)): We observe that, in both cases, for small t_0 and for a wide range of s_0 values, variations are strongly anticorrelated. More precisely, this implies that in panel (a), where only consecutive variations with the same positive sign are considered, the number of couples in the real catalog is smaller than the average number of couples in the reshuffled catalogs, for almost all s_0. This means that, at times shorter than 5 s, consecutive variations with the same positive sign are less frequent than in the uncorrelated case, i.e., such variations are anti-correlated. At longer temporal distances, variations become completely uncorrelated ($\delta P(s_0, t_0) = 0$), namely the probability to observe two successive variations with the same sign is the same as in a reshuffled catalog. Conversely, the analysis of variations with different signs provides interesting insights: for case (c), the quantity Δs is always positive and therefore $\delta P(s_0, t_0)$ is simply equal to zero for negative s_0. Conversely, for positive s_0 data show strong correlations rapidly decreasing with the temporal distance, namely it is probable that a local decrease in voxel activity is followed by an activity enhancement close in time. Since $\delta P(s_0, t_0)$ for $t_0 = 5$ s tends to a constant value for $s_0 \lesssim 300$, i.e., contributions from more couples do not arise for larger s_0. We can infer that typically successive activity variations tend to differ by a quantity smaller than $\simeq$300.

Strong correlations are also observed in case (d), where the quantity Δs is always negative and therefore $\delta P(s_0, t_0)$ assumes a constant value for the entire range of positive s_0. It is interesting to stress that this happens since the same number of couples contributes to the conditional probability evaluated in the real catalog. However this number is not necessarily equal to the average number obtained for reshuffled catalogs and therefore $\delta P(s_0, t_0) \neq 0$. In this case data suggest that a local increase

in activity induces, after a short delay, a successive activity depression. By extrapolating to zero $\delta P(s_0, t_0)$ for negative s_0, we find the s_0 value smaller than any variation recorded in the catalog. We then find that successive activity variations tend to differ by values larger than $\simeq -900$. In both cases correlations rapidly decrease in time and variations become uncorrelated over a temporal distance of about 100 s. The overall analysis suggests that successive activity enhancements or depressions are strongly unlikely if close in time and completely uncorrelated over longer temporal scales. Conversely, turning off activity in some voxels triggers activity enhancements in other voxels after a short time delay, and vice versa. Variations of different signs show, indeed, a stronger evidence of correlations suggesting that the system activity realizes a sort of homeostatic balance compensating local variations.

These results can be better enlightened by evaluating the derivative $\frac{d\delta P(s_0,t_0)}{ds_0}$, which represents the probability difference to observe $\Delta s = s_0$ conditioned to $\Delta t < t_0$ (Fig. 5). As expected, the total area underlying the four different cases of dP/ds_0 is zero. Also in this case, deviations with different signs are analyzed separately. As observed for Fig. 4, deviations with the same sign (case (a) and (b)), are strongly anticorrelated. Conversely, variations with opposite signs (case (c) and (d)) show clear evidence of correlations over a temporal scale of few seconds. Data confirm that the most probable value for successive variations difference is about 300 for case (c), whereas the most probable value is -600 for case (d). This value is larger than -900 as inferred from Fig. 4.

We have performed the same analysis imposing the condition on the voxel e Euclidean distance (Fig. 6). Concerning this point we need to specify that, since we are focusing our analysis of high activity voxels by imposing a threshold value B_c to $B(\vec{r}_i, t_i)$, we cannot explore the entire spatial range since for $B_c = 18{,}000$ the maximum distance observed for active voxels is about 70 mm. In this case, error bars are larger and therefore conclusions must be drawn more carefully. Variations with the same sign

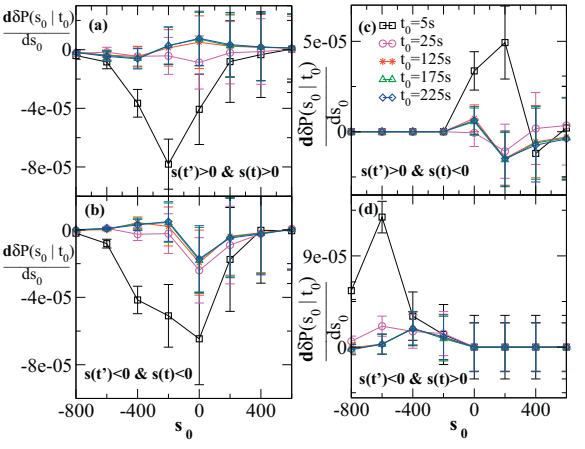

Fig. 5. The derivative $\frac{d\delta P(s_0,t_0)}{ds_0}$ as a function of s_0 for $t_0 = 5$, 25, 125, 175, 225 s. For each t_0 and s_0 the error bar is the standard deviation $\sigma(s_0, t_0)$. Different panels consider all possible combinations of sign of successive variations.

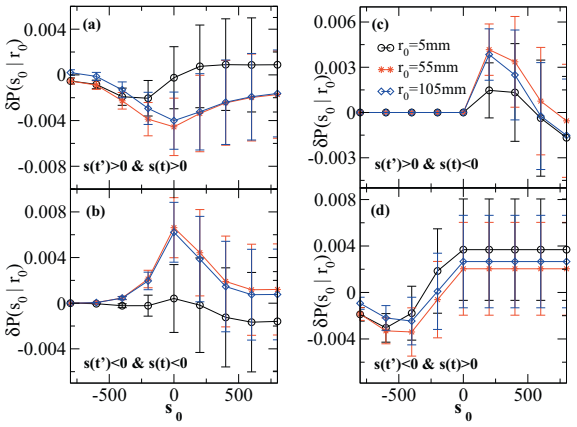

Fig. 6. The quantity $\delta P(s_0, r_0)$ as a function of s_0 for $r_0 = 5$, 55 and 105 mm. For each r_0 and s_0 the error bar is the standard deviation $\sigma(s_0, r_0)$. Different panels consider all possible combinations of sign of successive variations.

(case (a) and (b)) show an interesting behavior for $\delta P(s_0, r_0) \sim 0$: Successive positive variations appear to be mostly anticorrelated. Conversely it is likely to observe successive depressions in activity over distances on the cm scale. Since the maximum of $\delta P(s_0, r_0)$ is at $s_0 = 0$, these successive depressions tend to have the same amplitude. Data suggest that activity dampening propagates over neighboring voxels. On the other hand, variations with opposite sign (case (c)) give indication of correlation over an Euclidean distance up to 100 mm, the expected decay at longer distances is not measurable due to the poor statistics of data. Conversely, case (d) apparently suggests that a local small enhancement is likely followed by a depression within distances on the cm scale, whose sum of absolute values is in the range $]0, 200[$. However, data exhibit large error bars and therefore it is difficult to draw any clear conclusion. To clarify this point a more careful analysis is needed in order to decrease the error bars.

3. Discussion

This study was inspired by the farseeing work of Gerhard Werner who strongly supported the relevance of interdisciplinary approaches to the understanding of brain dynamics. Since 2003, when spontaneous activity in cortical slices was first found to follow scale-free statistical distributions in size and duration, increasing experimental evidences and theoretical models have been reported in the literature supporting the emergence of evidence of scale invariance in the cortex. Although strongly debated, such results refer to many different in vitro and in vivo preparations (awake monkeys, anesthetized rats and cats, in vitro slices and dissociated cultures), suggesting that power law distributions and scale free correlations are a very general and robust feature of cortical activity that has been conserved across species as specific substrate for information storage, transmission and processing. Equally important is that the features reminiscent of scale invariance and criticality are observed at scale spanning

from the level of interacting arrays of neurons all the way up to correlations across the entire brain. A fundamental feature of systems acting close to a critical point is the emergence of complex properties due to the interactions of many degrees of freedom. The existence of long-range spatio-temporal correlations in a system close to a critical point is a fundamental ingredient at the basis of complex behavior.

Here we make use of the analogy between energy release in earthquake occurrence and bursts of brain activity measured in fMRI signals. Attention is focused on records with large amplitude in analogy with observations in seismic occurrence: large earthquakes trigger a sequence of successive events whose rate decays in time as the Omori law and whose spatial location diffuses away from the mainshock epicenter. Our aim is to understand if variations in brain activity are simply driven by local mechanisms, or rather variations occurring close in time and space are able to affect the activity in a particular brain region. This question has indeed an even wider scope: The understanding of the temporal organization of activity can shed some light on the mechanisms organizing brain activity on a larger scale. For instance, the analysis of correlations in earthquake occurrence has shown that magnitudes of successive earthquakes are correlated, in particular the successive event tends to have a size close but smaller than the previous one. This feature is in perfect agreement with the picture of earthquake occurrence as a process redistributing elastic stress over a surrounding region leading to the occurrence of successive events. Other stochastic processes, for instance solar flares, while following similar statistical laws, exhibit temporal correlations with different features, namely the following flare tends to have a size close but larger than the previous one. In this process the physical mechanisms controlling magnetic energy release have different features [40].

The analysis performed on extreme events in BOLD signals suggests that activity variations with opposite sign, namely activity enhancements and depressions, are correlated in time at least over a temporal scale of some seconds. This result suggests that the system tends to realize an activity balance, where depressions are compensated by successive enhancements and vice versa. Interestingly, it is not observed that local enhancements in voxel activity trigger further enhancements after a time delay, as it could be simply expected from the propagation of activity at the level of individual neurons. Neither it is observed that depressions in activity induce further depressions. The analysis indicates an homeostatic balance in the activity as a mechanism controlling the temporal organization. From the point of view of the spatial correlations, the analysis is affected by stronger statistical noise and therefore conclusions are less evident. However, data suggest that the leading event is the depression in voxel activity which may induce both enhancement or further depression in neighboring voxels.

Appendix A. FMRI data acquisition and preprocessing

The human brain data discussed are taken from experiments previously reported [34]. Data were obtained, after informed consent, from seven healthy, right-handed human subjects (data used in this paper corresponds to Subject 1, set 4). They were recorded by a Siemens-Trio 3.0 Tesla imaging system using a birdcage radio-frequency head coil. Blood oxygenation level-dependent single-shot echo-planar T2-weighted imaging was obtained using scan repeat time of 2.5 s, echo time of 30 ms, flip angle 90, and field 256 mm. Data were preprocessed using the package FSL (http://www.fmrib.ox.ac.uk/fsl). Preprocessing of BOLD signal was performed using FMRIB Expert Analysis Tool (http://www.fmrib.ox.ac.uk/fsl), including motion correction using MCFLIRT, slice-timing correction using Fourier-space time-series phase-shifting, non-brain removal using BET and spatial smoothing using a Gaussian kernel of full-width-half-maximum 5 mm. All procedures employed were approved by Northwestern University Institutional Review Board.

References

[1] Fox MD, Raichle M. Nat Rev Neurosci 2007;8:700.
[2] Beckmann CF, DeLuca M, Devlin JT, Smith SM. Philos Trans R Soc London Ser B 2005;360:1001.
[3] Smith SM, Fox PT, Miller KL, Glahn DC, Fox PM, Mackay CE, Filippini N, Watkins KE, Toro R, Laird AR, Beckmann CF. Proc Natl Acad Sci USA 2009;106:13040.
[4] Bak P. How Nature Works: The Science of Self-organized Criticality. New York: Copernicus Books; 1996.
[5] Chialvo DR. Nat Phys 2010;6:744.
[6] Expert P, Lambiotte R, Chialvo DR, Christensen K, Jensen HJ, Sharp DJ, Turkheimer F. J R Soc Interface 2011;8:472.
[7] Tagliazucchi E, Balenzuela P, Fraiman D, Chialvo DR. Front Physiol 2012;3:15.
[8] Beggs JM, Plenz D. J Neurosci 2003;23:11167.
[9] Petermann T, Thiagarajan TC, Lebedev MA, Nicolelis MAL, Chialvo DR, Plenz D. Proc Natl Acad Sci USA 2009;106:15921.
[10] Thiagarajan TC, Lebedev MA, Nicolelis MAL, Plenz D. PLoS Biol 2010;8:e1000278.
[11] Fraiman D, Balenzuela P, Foss J, Chialvo DR. Phys Rev E 2009;79:061922.
[12] Kitzbichler MG, Smith ML, Christensen SR, Bullmore E. PLoS Comput Biol 2009;5:e1000314.
[13] Deco G, Jirsa V. J Neurosci 2012;32:3366.
[14] Haimovici A, Tagliazucchi E, Balenzuela P, Chialvo DR. Phys Rev Lett 2013;110:178101.
[15] de Arcangelis L, Perrone-Capano C, Herrmann HJ. Phys Rev Lett 2006;96:028107.
[16] Pellegrini GL, de Arcangelis L, Herrmann HJ, Perrone Capano C. Modelling. Phys Rev E 2007;76:016107.
[17] de Arcangelis L, Herrmann HJ. Proc Natl Acad Sci USA 2010;107:3977.
[18] Lombardi F, Herrmann HJ, Perrone-Capano C, Plenz D, de Arcangelis L. Phys Rev Lett 2012;108:228703.
[19] Beggs JM, Plenz D. J Neurosci 2004;24:5216.
[20] Gireesh ED, Plenz D. Proc Natl Acad Sci USA 2008;105:7576.
[21] Mazzoni A, Broccard FD, Garcia-Perez E, Bonifazi P, Ruaro ME, Torre V. PLoS One 2007;2:e439.
[22] Pasquale V, Massobrio P, Bologna LL, Chiappalone M, Martinoia S. Neuroscience 2008;153:1354.
[23] Shew WL, Yang H, Petermann T, Roy R, Plenz D. J Neurosci 2009;29:155595–600.
[24] Bak P, Tang C. J Geophys Res 1989;94:15635.
[25] Sornette A, Sornette D. Europhys Lett 1989;9:197.
[26] Bak P, Sneppen K. Phys Rev Lett 1993;71:4083.
[27] Lu ET, Hamilton RJ. Astrophys J 1991;380:L89.
[28] Politzer PA. Phys Rev Lett 2000;84:1192.
[29] Faillettaz J, Louchet F, Grasso JR. Phys Rev Lett 2004;93:208001.
[30] Peters O, Hertlein C, Christensen K. Phys Rev Lett 2002;88:018701.
[31] Werner G. Front Physiol 2010;1:1.
[32] Werner G. Cognit Neurodyn 2012;6:199.
[33] Chialvo DR. In: Cooperative behavior in neural systems: Ninth Granada Lectures. AIP Conference Proceedings, vol. 887. p. 1–12.

[34] Eguiluz VM, Chialvo DR, Cecchi G, Baliki M, Apkarian V. Phys Rev Lett 2005;94:018102.
[35] Bailey P, von Bonin G, McCulloch WS. The Isocortex of the Chimpanzee. Urbana USA: Univeristy of Illinois Press; 1950. pp. 1–440.
[36] Dusser de Barenne JG, Garol W, McCulloch WS. J Neurophysiol 1941;4:324.
[37] McCulloch WS. Physiol Rev 1944;24:390–407.
[38] Lippiello E, de Arcangelis L, Godano C. Phys Rev Lett 2008;100:038501.
[39] Tagliazucchi E, Balenzuela P, Fraiman D, Montoya P, Chialvo DR. Neurosci Lett 2011;488:158.
[40] Lippiello E, de Arcangelis L, Godano C. Astron and Astrophys 2010;511:L2.